

Explainability-Guided Defense: Attribution-Aware Model Refinement Against Adversarial Data Attacks

Longwei Wang[†], Mohammad Navid Nayyem[†], Abdullah Al Rakin[†], KC Santosh[†], Chaowei Zhang[‡],
and Yang Zhou[#]

[†]*AI Lab, Department of Computer Science, University of South Dakota, Vermillion, SD, USA*

[‡]*School of Information Engineering, Yangzhou University, Yangzhou, Jiangsu, China*

[#]*Department of CSSE, Auburn University, Auburn, AL, USA*

{longwei.wang | kc.santosh}@usd.edu, cwzhang@yzu.edu.cn, and yangzhou@auburn.edu

Abstract—The growing reliance on deep learning models in safety-critical domains such as healthcare and autonomous navigation underscores the need for defenses that are both robust to adversarial perturbations and transparent in their decision-making. In this paper, we identify a connection between interpretability and robustness that can be directly leveraged during training. Specifically, we observe that spurious, unstable, or semantically irrelevant features identified through Local Interpretable Model-Agnostic Explanations (LIME) contribute disproportionately to adversarial vulnerability. Building on this insight, we introduce an attribution-guided refinement framework that transforms LIME from a passive diagnostic into an active training signal. Our method systematically suppresses spurious features using feature masking, sensitivity-aware regularization, and adversarial augmentation in a closed-loop refinement pipeline. This approach does not require additional datasets or model architectures and integrates seamlessly into standard adversarial training. Theoretically, we derive an attribution-aware lower bound on adversarial distortion that formalizes the link between explanation alignment and robustness. Empirical evaluations on CIFAR-10, CIFAR-10-C, and CIFAR-100 demonstrate substantial improvements in adversarial robustness and out-of-distribution generalization.

Index Terms—Explainability, Adversarial Robustness, Interpretability, LIME, Data Attacks.

I. INTRODUCTION

Deep neural networks (DNNs) have revolutionized modern artificial intelligence, achieving state-of-the-art performance across a wide spectrum of applications, including image recognition, natural language processing, autonomous navigation, and medical diagnostics [1], [2]. Among these, convolutional neural networks (CNNs) have emerged as the cornerstone for visual perception tasks, owing to their ability to hierarchically extract and integrate spatial patterns through shared-weight architectures and local connectivity. Despite their remarkable capabilities, DNNs remain acutely vulnerable in adversarial and out-of-distribution (OOD) environments. A critical limitation is their susceptibility to adversarial examples—imperceptible perturbations carefully optimized to mislead models into making incorrect

and often high-confidence predictions [3], [4]. These perturbations exploit the model’s reliance on brittle and non-semantic features, reflecting the underlying instability of decision boundaries in high-dimensional spaces. Beyond adversarial attacks, recent studies have shown that DNNs frequently latch onto spurious correlations or shortcut cues—non-causal features that correlate with labels in the training data but fail under distributional shifts [5]. Such dependencies can severely undermine a model’s generalization and fairness, especially in safety-critical applications like healthcare and autonomous driving. Compounding these challenges is the opaque nature of modern deep learning models. Often characterized as “black boxes,” these models offer limited insight into the internal logic behind their predictions [6]. This opacity hampers model debugging, restricts regulatory compliance, and diminishes user trust, thereby constraining the deployment of AI in domains that demand accountability, transparency, and robustness.

To address these issues, explainable AI (XAI) methods such as Local Interpretable Model-Agnostic Explanations (LIME) [7] and SHapley Additive exPlanations (SHAP) [8] have emerged as powerful tools for attributing predictions to input features. These techniques expose model reasoning by generating instance-specific feature importance maps, which can reveal reliance on irrelevant or misleading patterns. However, most XAI methods are used retrospectively—they analyze trained models without influencing the training process itself. As a result, a critical opportunity remains untapped: using attribution feedback to actively guide learning away from spurious features during model optimization.

While adversarial training is a widely adopted defense mechanism, it often acts as a brute-force solution, lacking interpretability and failing to provide insights into how and why robustness is achieved. Recent empirical findings, however, suggest a deeper connection: robust models tend to produce more stable and semantically aligned explanations, while non-robust models exhibit scattered

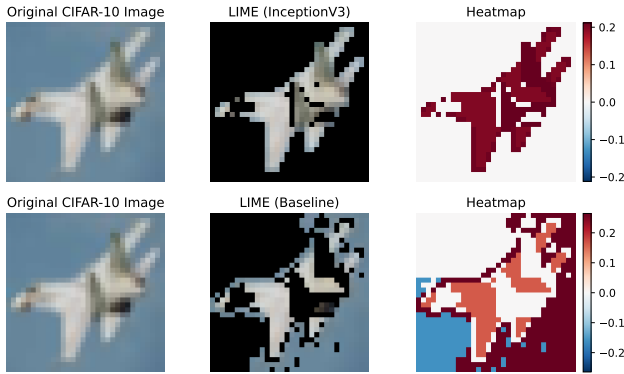


Fig. 1: LIME-based feature attribution maps illustrating the difference in learned representations between robust and non-robust models. The robust model (InceptionV3) consistently attends to semantically meaningful regions, while the non-robust baseline focuses on irrelevant or noise-sensitive areas.

or spurious attribution patterns [9], [10]. This relationship is visually demonstrated in Figure 1, where robust models consistently attend to task-relevant features. These insights motivate a paradigm shift—moving beyond reactive robustness toward proactive, explanation-aware training.

In this paper, we propose a novel training framework that operationalizes this insight by embedding explainability directly into the adversarial learning pipeline. Specifically, we introduce an attribution-aware refinement architecture that transforms LIME from a post-hoc explanation tool into a functional training signal. Our framework identifies semantically irrelevant, overly sensitive, or unstable features using LIME attributions and systematically suppresses their influence through a triad of mechanisms: (1) input-level feature masking, (2) sensitivity-aware gradient regularization, and (3) targeted adversarial training. This closed-loop architecture iteratively recalibrates the model’s attention, aligning learned representations with robust, semantically grounded features. Our central hypothesis is that interpretability and robustness are mutually reinforcing. Models that ground predictions in interpretable and stable features are less susceptible to adversarial manipulation, while robust models in turn produce more faithful and reliable explanations. We formalize this intuition by deriving an attribution-aware lower bound on adversarial distortion using a masked gradient formulation inspired by local Lipschitz continuity. Empirically, we show that our framework enhances both robustness and attributional clarity across a range of evaluation settings. The key contributions of this work are summarized below:

- We propose a unified defense framework that transforms interpretability into an active training signal,

systematically reducing spurious feature dependencies via LIME-guided model refinement.

- We introduce a theoretical robustness analysis based on attribution-aligned gradient suppression and local Lipschitz bounds, establishing formal links between interpretability and adversarial resilience.
- We conduct extensive experiments on CIFAR-10, CIFAR-10-C, and CIFAR-100 demonstrating substantial improvements in adversarial robustness and attributional quality without compromising clean accuracy.

II. RELATED WORKS

A. Adversarial Robustness in Deep Models

Convolutional neural networks (CNNs) are known to be vulnerable to adversarial perturbations—carefully crafted, imperceptible changes to input data that can mislead the model into making incorrect predictions [11], [12]. Foundational attacks such as the Fast Gradient Sign Method (FGSM) [3] and Projected Gradient Descent (PGD) [4] have prompted the development of a variety of defenses, most notably adversarial training [4], [13]–[15] and preprocessing-based sanitization methods [16].

Although effective, these approaches often incur substantial computational costs and may generalize poorly across different attack types [15], [17], [18]. More importantly, they are typically agnostic to the model’s internal reasoning and provide little insight into whether the learned representations are semantically meaningful or aligned with human intuition.

B. Model Interpretability

Interpretability methods aim to provide insight into the decision-making processes of complex models. Popular tools such as Local Interpretable Model-Agnostic Explanations (LIME) [7] and SHapley Additive exPlanations (SHAP) [8] attribute importance scores to input features based on their contribution to the model’s output. Visual explanation techniques such as Grad-CAM [19] and Integrated Gradients [20] have further enhanced the interpretability of CNNs, particularly in vision tasks.

However, most of these techniques are employed post hoc and play no role in the training process [21] [22]–[25]. Consequently, while they are useful for diagnosing spurious behavior or identifying misleading dependencies, they do not directly contribute to improving model robustness. Our work departs from this passive paradigm by actively integrating LIME into the training loop to guide attention control and improve robustness.

C. Integrating Interpretability and Robustness

There is growing recognition that interpretability can play a pivotal role in achieving robust deep learning [26] [27] [28], [29] [30], [31]. Doshi-Velez and Kim [32] suggested that aligning models with human-interpretable

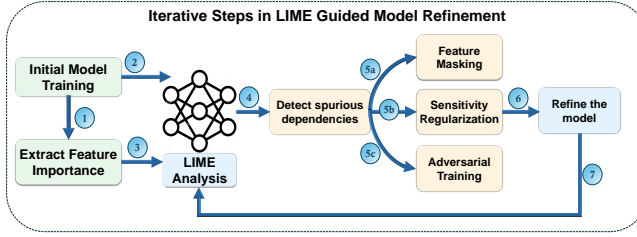


Fig. 2: Overview of the iterative XAI-guided refinement framework. LIME highlights spurious features post initial training. These are mitigated through feature masking, sensitivity regularization, and adversarial training. The process iterates until robustness and interpretability metrics converge.

features may help avoid reliance on spurious patterns. Adebayo et al. [33] proposed sanity checks to evaluate the reliability of saliency maps, while Slack et al. [34] showed that explanation tools like LIME and SHAP are themselves vulnerable to adversarial manipulation.

Ross and Doshi-Velez [9] demonstrated that incorporating gradient-based interpretability constraints into the loss function can improve adversarial robustness. Similarly, Dombrowski et al. [35] studied how adversarial robustness affects the stability of feature attribution maps. While these studies highlight a conceptual link between robustness and interpretability [36] [37], they stop short of proposing a unified training framework that exploits this relationship for model refinement.

III. METHODOLOGY

To bridge interpretability and robustness, we introduce a unified framework that integrates explainable AI (XAI) into the training loop of deep neural networks for targeted model refinement under adversarial conditions. At the core of our approach is the use of Local Interpretable Model-Agnostic Explanations (LIME) to identify spurious, unstable, or semantically irrelevant features that compromise robustness. Rather than using interpretability tools as passive diagnostics, we transform them into active refinement signals that guide an iterative training process involving feature masking, sensitivity regularization, and adversarial augmentation. As shown in Fig. 2, the process is cyclic and designed to promote semantic consistency, attributional stability, and gradient robustness over successive refinements.

A. Attribution-Guided Analysis

To assess feature-level relevance, we apply LIME to construct local surrogate models around each input x . Let $\mathcal{Z} = \{(z_i, f(z_i))\}_{i=1}^N$ be a set of perturbed inputs obtained by masking subsets of x , and let:

$$w_i = \exp\left(-\frac{\|x - z_i\|_2^2}{\sigma^2}\right) \quad (1)$$

be a locality-aware kernel. A linear surrogate model $g(z) = \beta_0 + \sum_{j=1}^d \beta_j z_j$ is trained by minimizing the weighted squared loss:

$$\mathcal{L}_{\text{surrogate}} = \sum_{i=1}^N w_i (f(z_i) - g(z_i))^2. \quad (2)$$

The resulting attribution vector β serves as a feature-level explanation of the model's decision. The absolute attribution $|\beta_j|$ quantifies the importance of input feature x_j :

$$\text{Importance}(x_j) = |\beta_j|. \quad (3)$$

B. Spurious Feature Identification

Not all highly attributed features are beneficial for robustness. We define features as *spurious* if they exhibit at least one of the following undesirable traits:

(1) Irrelevance: A feature is deemed irrelevant if it receives disproportionately high attribution from LIME despite lacking semantic relevance. To distinguish relevant from irrelevant attributions, we leverage a reference model with higher interpretability—specifically, a well-trained ResNet-50—as a proxy for identifying class-relevant features. We then compare the LIME attribution maps of our baseline model against those of the reference model to assess alignment with the true class semantics. A feature is flagged as irrelevant if it exceeds a predefined attribution magnitude threshold:

$$|\beta_j| > \tau, \quad (4)$$

where β_j denotes the LIME attribution score for feature x_j . Features satisfying this condition but not supported by the reference model are considered spurious and targeted for suppression in the refinement process.

(2) Sensitivity: Features with excessively high input gradients can cause disproportionate changes in the model's output under small perturbations. To quantify this behavior, we define the sensitivity of a feature x_j as the magnitude of its input gradient:

$$\text{Sensitivity}(x_j) = \left| \frac{\partial f(x)}{\partial x_j} \right| > \epsilon, \quad (5)$$

where ϵ is a predefined sensitivity threshold. To ensure that gradient magnitude aligns with semantic relevance, we additionally compare feature sensitivities with those from a reference model (e.g., a well-trained ResNet-50) known for producing more interpretable attributions. If a feature exhibits high sensitivity in the baseline model but lacks corresponding importance in the reference model, it is considered semantically ungrounded and is subsequently targeted for regularization during the model refinement process.

(3) Instability: Features whose attributions vary significantly under input perturbations are considered un-

stable. Attribution instability is defined as the variance of LIME importance scores across N perturbed samples:

$$\text{Instability}(x_j) = \text{Var} \left(\left\{ \beta_j^{(i)} \right\}_{i=1}^N \right) > \delta, \quad (6)$$

where δ is an instability threshold. A feature is classified as spurious if it satisfies at least one of the above conditions:

$$x_j \in \mathcal{F}_{\text{spurious}} \iff |\beta_j| > \tau \vee \text{Sensitivity}(x_j) > \epsilon \vee \text{Instability}(x_j) > \delta. \quad (7)$$

C. XAI-Guided Model Refinement

1) Feature Masking

We suppress the influence of spurious features using a binary mask $m \in \{0, 1\}^d$, where:

$$m_j = \begin{cases} 0 & \text{if } x_j \in \mathcal{F}_{\text{spurious}}, \\ 1 & \text{otherwise.} \end{cases} \quad (8)$$

The masked input is then

$$x^{\text{masked}} = x \odot m. \quad (9)$$

2) Sensitivity Regularization

To penalize over-reliance on unstable features, we introduce a sensitivity regularization term. The composite loss becomes:

$$\mathcal{L}_{\text{total}} = \mathcal{L}_{\text{task}} + \lambda \cdot \mathcal{L}_{\text{reg}}, \quad (10)$$

where:

$$\mathcal{L}_{\text{task}} = -\frac{1}{n} \sum_{i=1}^n \sum_{k=1}^K y_{ik} \log f_k(x_i), \quad (11)$$

$$\mathcal{L}_{\text{reg}} = \frac{1}{|\mathcal{F}_{\text{spurious}}|} \sum_{j \in \mathcal{F}_{\text{spurious}}} \left\| \frac{\partial f(x)}{\partial x_j} \right\|^2. \quad (12)$$

3) Adversarial Training

To reinforce robustness, we include adversarial examples generated using FGSM:

$$x^{\text{adv}} = x + \epsilon \cdot \text{sign}(\nabla_x \mathcal{L}_{\text{task}}(f(x), y)), \quad (13)$$

and compute adversarial loss:

$$\mathcal{L}_{\text{adv}} = \mathbb{E}_{(x,y) \sim \mathcal{D}} [\mathcal{L}_{\text{task}}(f(x^{\text{adv}}), y)]. \quad (14)$$

The final training objective integrates all three components:

$$\mathcal{L}_{\text{total}} = \mathcal{L}_{\text{task}} + \alpha \cdot \mathcal{L}_{\text{adv}} + \lambda \cdot \mathcal{L}_{\text{reg}}. \quad (15)$$

D. Iterative Refinement Procedure

The training proceeds iteratively as shown in **Algorithm 1**. In each iteration, the model is updated using the composite loss, LIME attributions are recomputed, and spurious features are re-evaluated. The process converges when robustness metrics stabilize or when attribution maps exhibit consistent, class-relevant focus across perturbations. This iterative loop ensures that the model increasingly grounds its predictions in robust, interpretable features—bridging the divide between adversarial defense and attributional transparency.

Algorithm 1 XAI-Guided Model Refinement for Enhanced Adversarial Robustness

INPUT: Initial model f_θ , training data \mathcal{D} , feature attribution model LIME, thresholds (τ, ϵ, δ) , and hyperparameters (λ, α) .

OUTPUT: Refined robust model f_θ^* .

Notations: $\mathcal{F}_{\text{spurious}}$: Set of flagged spurious features, $\mathcal{L}_{\text{task}}$: task-specific loss, \mathcal{L}_{adv} : adversarial loss, \mathcal{L}_{reg} : sensitivity regularization loss.

```

1: Initialize model  $f_\theta$  using standard training on  $\mathcal{D}$ 
2: repeat
3:    $A \leftarrow \text{FEATUREATTRIBUTION}(f_\theta, \mathcal{D}, \text{LIME})$ 
4:    $\mathcal{F}_{\text{spurious}} \leftarrow \text{IDENTIFYSPURIOUSFEATURES}(A, f_\theta, \tau, \epsilon, \delta)$ 
5:   Apply refinement strategies:
6:     • FEATUREMASKING( $\mathcal{F}_{\text{spurious}}, \mathcal{D}$ )
7:     • SENSITIVITYREGULARIZATION( $f_\theta, \mathcal{F}_{\text{spurious}}, \lambda$ )
8:     • ADVERSARIALTRAINING( $f_\theta, \mathcal{D}, \alpha$ )
9:   Re-train model  $f_\theta$  with updated loss:

$$\mathcal{L} = \mathcal{L}_{\text{task}} + \alpha \cdot \mathcal{L}_{\text{adv}} + \lambda \cdot \mathcal{L}_{\text{reg}}$$

10:  until Convergence or robustness constraint is satisfied
11:  return  $f_\theta^*$ 

```

IV. THEORETICAL ANALYSIS: BRIDGING INTERPRETABILITY AND ROBUSTNESS

This section establishes a formal connection between interpretability and adversarial robustness through the lens of feature attribution, gradient sensitivity, and decision boundary smoothness. Drawing inspiration from robustness theory—particularly Lipschitz-based analyses such as CLEVER [38]—we demonstrate how the proposed explainability-guided attention control framework reduces adversarial vulnerability by suppressing sensitivity to spurious features identified via LIME.

A. Attribution-Constrained Model Behavior

Let $f : \mathbb{R}^d \rightarrow \mathbb{R}^K$ be a multi-class classifier mapping input vectors $x \in \mathbb{R}^d$ to output logits $f_1(x), \dots, f_K(x)$. The predicted class is $y = \arg \max_k f_k(x)$. An adversarial example is defined as a perturbed input $x + \delta$ such that $\arg \max_k f_k(x + \delta) \neq y$, with $\|\delta\|_p \leq \epsilon$.

For differentiable models, the first-order Taylor expansion yields:

$$f_k(x + \delta) \approx f_k(x) + \langle \nabla_x f_k(x), \delta \rangle. \quad (16)$$

The change in prediction can be bounded using the norm of the gradient [39] [40]:

$$\sup_{\|\delta\|_p \leq \epsilon} |f_y(x) - f_j(x + \delta)| \leq \epsilon \cdot \|\nabla_x(f_y(x) - f_j(x))\|_q, \quad (17)$$

where $\|\cdot\|_q$ is the dual norm of $\|\cdot\|_p$.

This sensitivity motivates the use of gradient regularization as a defense mechanism. However, instead of regularizing all features equally, we aim to regularize spurious features—those identified by LIME as irrelevant, unstable, or highly sensitive.

B. Attribution-Aligned Gradient Suppression

Let $\beta_j(x)$ be the LIME attribution for feature x_j . Define the normalized attribution vector:

$$a(x) = \frac{[\|\beta_1(x)\|, \dots, \|\beta_d(x)\|]}{\sum_{j=1}^d |\beta_j(x)|}. \quad (18)$$

The directional alignment between model gradients and attribution is given by:

$$\text{Align}(x) = \frac{\langle \nabla_x f_y(x), a(x) \rangle}{\|\nabla_x f_y(x)\|_2 \cdot \|a(x)\|_2}. \quad (19)$$

A low alignment implies that the model's gradient sensitivity is dominated by features not identified as important—an indicator of vulnerability to adversarial perturbations.

C. Attribution-Aware Lower Bound on Adversarial Distortion

We now formalize the relationship between attribution-driven feature selection and adversarial robustness by introducing an attribution-aware lower bound on the minimum adversarial distortion required to change the model's prediction. This bound draws on the concept of local Lipschitz continuity [39] [41] while incorporating constraints derived from LIME-based feature attribution and sensitivity analysis.

Let $f : \mathbb{R}^d \rightarrow \mathbb{R}^K$ be a classifier that is locally Lipschitz continuous with constant L_q in the ℓ_p norm. Let $x \in \mathbb{R}^d$ be an input sample with true label $y = \arg \max_k f_k(x)$. Define $\mathcal{F}_{\text{spurious}} \subset \{1, \dots, d\}$ as the set of features identified via LIME as spurious—i.e., features exhibiting high attribution magnitude, high gradient sensitivity, or instability across perturbed neighborhoods.

Suppose that for all $j \in \mathcal{F}_{\text{spurious}}$, the following conditions hold:

$$|\beta_j(x)| \leq \tau, \quad (20)$$

$$\left| \frac{\partial f_y(x)}{\partial x_j} \right| \leq \epsilon, \quad (21)$$

where τ and ϵ are small, user-defined thresholds for attribution and sensitivity respectively. Then, for any untargeted adversarial attack constrained within an ℓ_p ball of radius δ , the minimum perturbation required to change the prediction satisfies:

$$\Delta_{\min}(x) \geq \min_{j \neq y} \frac{f_y(x) - f_j(x)}{L_q^{\text{eff}}(x)}, \quad (22)$$

where the effective Lipschitz constant is:

$$L_q^{\text{eff}}(x) = \|\nabla_x f_y(x) \odot (1 - m_{\text{spurious}})\|_q, \quad (23)$$

and $m_{\text{spurious}} \in \{0, 1\}^d$ is a binary mask such that:

$$m_{\text{spurious},j} = \begin{cases} 1, & \text{if } j \in \mathcal{F}_{\text{spurious}}, \\ 0, & \text{otherwise.} \end{cases} \quad (24)$$

Let us begin with the first-order Taylor expansion of the output logits:

$$f_k(x + \delta) \approx f_k(x) + \langle \nabla_x f_k(x), \delta \rangle. \quad (25)$$

For an untargeted attack to succeed, there must exist some $j \neq y$ such that:

$$f_j(x + \delta) \geq f_y(x + \delta). \quad (26)$$

Using the above expansion, the difference in logits becomes:

$$f_y(x + \delta) - f_j(x + \delta) \approx f_y(x) - f_j(x) + \langle \nabla_x (f_y(x) - f_j(x)), \delta \rangle. \quad (27)$$

To flip the prediction, it suffices to consider:

$$\langle \nabla_x (f_y(x) - f_j(x)), \delta \rangle \leq f_j(x) - f_y(x). \quad (28)$$

Applying Hölder's inequality, we obtain:

$$|\langle \nabla_x (f_y(x) - f_j(x)), \delta \rangle| \leq \|\nabla_x (f_y(x) - f_j(x))\|_q \cdot \|\delta\|_p. \quad (29)$$

Solving for the minimal norm of δ that satisfies the inequality leads to:

$$\|\delta\|_p \geq \frac{f_y(x) - f_j(x)}{\|\nabla_x (f_y(x) - f_j(x))\|_q}. \quad (30)$$

Now, assuming the spurious gradients are bounded by ϵ , and attribution scores satisfy the irrelevance constraint $|\beta_j(x)| \leq \tau$, we suppress these components by zeroing them out in the gradient vector using the mask m_{spurious} . Thus, we compute the effective Lipschitz constant:

$$L_q^{\text{eff}}(x) = \|\nabla_x f_y(x) \odot (1 - m_{\text{spurious}})\|_q. \quad (31)$$

This above analysis establishes that spurious features—those with high attribution scores but low semantic relevance or unstable importance—contribute to adversarial vulnerability by inflating the local gradient norm. By systematically identifying and suppressing such features via LIME-guided refinement (i.e., through masking and regularization), the model effectively reduces its sensitivity to adversarial perturbations. As a result, the effective Lipschitz constant $L_q^{\text{eff}}(x)$ becomes smaller, yielding a higher lower bound on the minimum adversarial distortion $\Delta_{\min}(x)$.

V. EXPERIMENTS AND DISCUSSIONS

A. Experiments Setup

To evaluate the effectiveness of our proposed framework—*Bridging Interpretability and Robustness through XAI-Guided Model Refinement*—we perform a comprehensive set of experiments across multiple datasets, model architectures, and adversarial threat models. The primary objective is to demonstrate that integrating LIME-based feature attribution into the model refinement loop enhances adversarial robustness and generalization without significantly degrading standard accuracy.

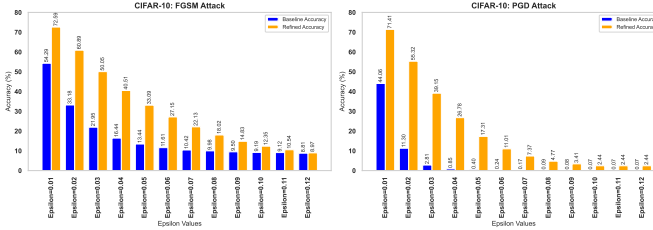


Fig. 3: Robustness Analysis under FGSM and PGD Attacks on CIFAR-10. The refined model consistently demonstrates improved performance across different perturbation strengths.

1) Datasets

We conduct experiments on three benchmark datasets that collectively provide a diverse evaluation setting: CIFAR-10, CIFAR-10-C and CIFAR-100.

2) Model Architectures

We adopt ResNet-18 [2] as our base architecture due to its balance between performance and computational efficiency. Its skip connections enable stable training, while its widespread adoption ensures comparability with prior work in adversarial robustness.

3) Adversarial Attack Configurations

To evaluate the robustness of our models under adversarial conditions, we consider three distinct evaluation scenarios: two involving gradient-based adversarial attacks (FGSM and PGD) and one targeting robustness to natural distributional shifts.

In addition to adversarial perturbations, we also evaluate the model’s robustness to natural distribution shifts using the CIFAR-10-C dataset. This dataset includes 19 types of common corruptions (e.g., noise, blur, weather, digital artifacts), each applied at five levels of severity. The goal of this evaluation is to assess the model’s out-of-distribution (OOD) generalization capacity and its ability to remain robust under realistic perturbations.

B. Experimental Results

1) CIFAR-10 Dataset

Fig. 3 highlights significant robustness improvements achieved by the refined model. Under FGSM attacks, the refined model retains 72.59% accuracy at $\epsilon = 0.01$ (compared to 54.29% for the baseline) and 50.05% at $\epsilon = 0.03$ (versus 21.95%). Similarly, for PGD attacks, the refined model achieves 71.41% accuracy at $\epsilon = 0.01$, substantially outperforming the baseline’s 44.06%.

2) CIFAR-100 Dataset

As shown in Fig. 4, the refined model demonstrates improved robustness on the more complex CIFAR-100 dataset. It achieves 43.55% FGSM accuracy at $\epsilon = 0.01$ (compared to 30.41% for the baseline) and 24.62% at $\epsilon = 0.03$ (versus 11.38%). For PGD attacks, the refined model achieves 41.96% accuracy at $\epsilon = 0.01$, significantly outperforming the baseline’s 23.06%.

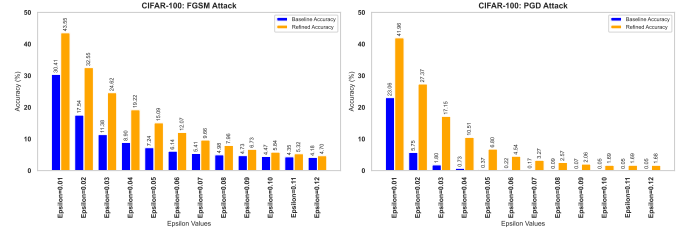


Fig. 4: Robustness Analysis under FGSM and PGD Attacks on CIFAR-100. The refined model consistently achieves improved performance across varying perturbation strengths.

3) CIFAR-10-C Dataset

Table I further highlights the robustness of the refined model, particularly against noise-based corruptions. The refined model sustains $>90\%$ accuracy under FGSM attacks at $\epsilon = 0.01$ and $>85\%$ under stronger PGD attacks. Cells highlighted in blue represent substantial gains ($>50\%$ over baseline), while red highlights indicate vulnerabilities ($<5\%$ accuracy). Across all corruption categories—noise, blur, and environmental—the refined model consistently achieves higher mean accuracy (87.15% versus 70.30% for FGSM and 84.81% versus 50.47% for PGD at $\epsilon = 0.01$) with lower variability, indicating greater stability.

VI. CONCLUSION

We proposed an attribution-guided training framework that integrates LIME explanations into the adversarial learning process to enhance model robustness and interpretability. By suppressing spurious and unstable features through masking, gradient regularization, and adversarial training, our method encourages reliance on semantically meaningful features. Experiments on CIFAR-10, CIFAR-10-C, and CIFAR-100 demonstrate improved adversarial robustness and generalization with minimal loss in clean accuracy. Visualization and ablation studies confirm that our refinement approach leads to more stable and interpretable model behavior. A theoretical analysis supports the connection between attribution alignment and adversarial resilience via an attribution-aware Lipschitz bound. Future work will explore alternative XAI methods, broader architectures, and applications in fairness-critical domains.

REFERENCES

- [1] A. Krizhevsky, I. Sutskever, and G. E. Hinton, “Imagenet classification with deep convolutional neural networks,” in *Advances in Neural Information Processing Systems (NeurIPS)*, 2012, pp. 1097–1105.
- [2] K. He, X. Zhang, S. Ren, and J. Sun, “Deep residual learning for image recognition,” in *Proceedings of the IEEE Conference on Computer Vision and Pattern Recognition (CVPR)*, 2016, pp. 770–778.
- [3] I. J. Goodfellow, J. Shlens, and C. Szegedy, “Explaining and harnessing adversarial examples,” in *International Conference on Learning Representations (ICLR)*, 2015.

TABLE I: Adversarial Robustness Analysis Against Common Corruptions on CIFAR-10-C

	$\epsilon = 0.01$				$\epsilon = 0.02$				$\epsilon = 0.03$			
	FGSM		PGD		FGSM		PGD		FGSM		PGD	
Corruption	Base	Ref	Base	Ref	Base	Ref	Base	Ref	Base	Ref	Base	Ref
Noise-Based												
Gaussian	79.06	90.69	65.87	90.32	43.4	88.54	13.68	86.57	25.17	86.13	3.29	71.44
Shot	79.58	90.63	65.97	90.32	43.39	88.16	14.25	85.84	24.49	85.61	2.75	68.18
Impulse	82.17	90.21	73.72	89.88	48.75	87.77	19.42	86.14	27.59	85.58	4.64	71.91
Speckle	80.53	90.69	67.96	90.38	45.28	88.13	15.08	86.44	26.05	85.94	3.24	71.21
Blur-Based												
Defocus	68.56	89.64	42.16	89.34	35.51	87.27	4.62	84.35	22.45	84.94	0.84	64.68
Glass	77.22	89.27	59.80	88.76	42.42	86.89	9.6	84.19	24.32	84.43	1.67	66.14
Motion	66.76	89.24	39.02	88.90	34.77	86.96	3.94	84.41	22.56	84.9	0.62	65.6
Zoom	67.40	90.03	41.50	89.60	34.36	87.39	3.98	84.49	21.78	85.06	0.62	64.2
Gaussian	66.27	88.10	37.28	87.27	33.68	84.22	3.51	76.63	22.35	79	0.54	53.06
Environmental												
Snow	78.18	90.17	63.03	89.78	43.39	87.92	12.12	86.04	25.66	85.82	2.26	70.16
Frost	69.37	89.41	44.39	88.80	31.68	86.99	4.8	82.19	17.23	84.49	1.04	56.66
Fog	28.49	57.69	4.98	34.31	10.64	57.08	0.09	7.42	6.84	57.48	0	2.01
Mean	70.30	87.15	50.47	84.81	37.27	84.78	8.76	77.89	22.21	82.45	1.79	60.44
Std	± 13.87	± 8.91	± 18.55	± 15.25	± 9.60	± 8.42	± 5.78	± 21.41	± 5.29	± 7.74	± 1.37	± 18.48

[†] Bold numbers indicate best performance for each corruption type and attack

Blue highlighting indicates significant improvement (>50%) over baseline

Red highlighting indicates critical vulnerability (<5% accuracy)

- [4] A. Madry, A. Makelov, L. Schmidt, D. Tsipras, and A. Vladu, "Towards deep learning models resistant to adversarial attacks," in *International Conference on Learning Representations (ICLR)*, 2018.
- [5] R. Geirhos, P. Rubisch, and C. M. et al., "Shortcut learning in deep neural networks," *Nature Machine Intelligence*, vol. 2, pp. 665–673, 2019.
- [6] W. Samek, T. Wiegand, and K.-R. Müller, "Explainable artificial intelligence: Understanding, visualizing and interpreting deep learning models," *ITU Journal: ICT Discoveries*, vol. 1, no. 1, pp. 39–48, 2017.
- [7] M. T. Ribeiro, S. Singh, and C. Guestrin, "Why should i trust you? explaining the predictions of any classifier," in *Proceedings of the ACM SIGKDD International Conference on Knowledge Discovery and Data Mining (KDD)*, 2016.
- [8] S. M. Lundberg and S.-I. Lee, "A unified approach to interpreting model predictions," in *Advances in Neural Information Processing Systems (NeurIPS)*, 2017.
- [9] A. S. Ross and F. Doshi-Velez, "Improving the adversarial robustness and interpretability of deep neural networks by regularizing their input gradients," 2018.
- [10] A.-K. Dombrowski, M. Alber, and C. J. A. et al., "Explanations can be manipulated and still be faithful: The case of feature attribution," 2019.
- [11] C. Szegedy, W. Zaremba, and I. S. et al., "Intriguing properties of neural networks," in *International Conference on Learning Representations (ICLR)*, 2014.
- [12] M. Zhu, S. Wei, H. Zha, and B. Wu, "Neural polarizer: A lightweight and effective backdoor defense via purifying poisoned features," *Advances in Neural Information Processing Systems*, vol. 36, 2024.
- [13] A. Zou, L. Phan, J. Wang, D. Duenas, M. Lin, M. Andriushchenko, J. Z. Kolter, M. Fredrikson, and D. Hendrycks, "Improving alignment and robustness with circuit breakers," in *The Thirty-eighth Annual Conference on Neural Information Processing Systems*, 2024.
- [14] L. Wang, I. I. Uddin, K. Santosh, C. Zhang, X. Qin, and Y. Zhou, "Bridging symmetry and robustness: On the role of equivariance in enhancing adversarial robustness," *arXiv preprint arXiv:2510.16171*, 2025.
- [15] L. Wang, A. Ghimire, K. Santosh, Z. Zhang, and X. Li, "Enhanced robustness by symmetry enforcement," *IEEE CAI*, 2024.
- [16] T. Qin, X. Gao, J. Zhao, K. Ye, and C.-z. Xu, "Apbench: A unified availability poisoning attack and defenses benchmark," *Transactions on Machine Learning Research*, 2024.
- [17] R. N. Ranabhat, L. Wang, X. Qin, Y. Zhou, and K. Santosh, "Multi-scale unrectified push-pull with channel attention for enhanced corruption robustness," in *Proceedings of the AAAI Symposium Series*, vol. 6, no. 1, 2025, pp. 34–41.
- [18] L. Wang, X. Li, and Z. Zhang, "Dense cross-connected ensemble convolutional neural networks for enhanced model robustness," *arXiv preprint arXiv:2412.07022*, 2024.
- [19] R. R. Selvaraju, M. Cogswell, A. Das, R. Vedantam, D. Parikh, and D. Batra, "Grad-cam: Visual explanations from deep networks via gradient-based localization," in *Proceedings of the IEEE International Conference on Computer Vision (ICCV)*, 2017, pp. 618–626.
- [20] M. Sundararajan, A. Taly, and Q. Yan, "Axiomatic attribution for deep networks," in *Proceedings of the 34th International Conference on Machine Learning (ICML)*, 2017, pp. 3319–3328.
- [21] S. Wang, M. A. Qureshi, L. Miralles-Pechuán, T. Huynh-The, T. R. Gadekallu, and M. Liyanage, "Explainable ai for 6g use cases: Technical aspects and research challenges," *IEEE Open Journal of the Communications Society*, 2024.
- [22] M. Ennab and H. Mccheick, "Advancing ai interpretability in medical imaging: A comparative analysis of pixel-level interpretability and grad-cam models," *Machine Learning and Knowledge Extraction*, vol. 7, no. 1, p. 12, 2025.
- [23] L. Wang and Q. Liang, "Representation learning and nature encoded fusion for heterogeneous sensor networks," *IEEE Access*, vol. 7, pp. 39 227–39 235, 2019.
- [24] C. Wall, L. Wang, R. Rizk, and K. Santosh, "Winsor-cam: Human-tunable visual explanations from deep networks via layer-wise winsorization," *arXiv preprint arXiv:2507.10846*, 2025.
- [25] I. I. Uddin, L. Wang, and K. Santosh, "Expert-guided explainable few-shot learning for medical image diagnosis," in *MICCAI Workshop on Data Engineering in Medical Imaging*. Springer Nature Switzerland Cham, 2025, pp. 95–104.
- [26] B. Chander, C. John, L. Warrier, and K. Gopalakrishnan, "Toward trustworthy artificial intelligence (tai) in the context of explain-

ability and robustness," *ACM Computing Surveys*, vol. 57, no. 6, pp. 1–49, 2025.

[27] P. Seth and V. K. Sankarapu, "Bridging the gap in xai-why reliable metrics matter for explainability and compliance," *arXiv preprint arXiv:2502.04695*, 2025.

[28] L. Wang, C. Wang, Y. Li, and R. Wang, "Explaining the behavior of neuron activations in deep neural networks," *Ad Hoc Networks*, vol. 111, p. 102346, 2021.

[29] S. K. Jagatheesaperumal, M. Rahouti, A. Alfatemi, N. Ghani, V. K. Quy, and A. Chehri, "Enabling trustworthy federated learning in industrial iot: bridging the gap between interpretability and robustness," *IEEE Internet of Things Magazine*, vol. 7, no. 5, pp. 38–44, 2024.

[30] L. Wang, I. I. Uddin, X. Qin, Y. Zhou, and K. Santosh, "Explainability-driven defense: Grad-cam-guided model refinement against adversarial threats," in *Proceedings of the AAAI Symposium Series*, vol. 6, no. 1, 2025, pp. 49–57.

[31] N. Nayyem, A. Rakin, and L. Wang, "Bridging interpretability and robustness using lime-guided model refinement," *arXiv preprint arXiv:2412.18952*, 2024.

[32] F. Doshi-Velez and B. Kim, "Towards a rigorous science of interpretable machine learning," *arXiv preprint arXiv:1702.08608*, 2017.

[33] J. Adebayo, J. Gilmer, and M. M. et al., "Sanity checks for saliency maps," in *Advances in Neural Information Processing Systems (NeurIPS)*, 2018.

[34] D. Slack, S. Hilgard, and E. J. et al., "Fooling lime and shap: Adversarial attacks on post hoc explanation methods," in *Proceedings of the AAAI/ACM Conference on AI, Ethics, and Society (AIES)*, 2020.

[35] Y. Zhou, S. Booth, M. T. Ribeiro, and J. Shah, "Do feature attribution methods correctly attribute features?" in *Proceedings of the AAAI conference on artificial intelligence*, vol. 36, no. 9, 2022, pp. 9623–9633.

[36] E. ŞAHİN, N. N. Arslan, and D. Özdemir, "Unlocking the black box: an in-depth review on interpretability, explainability, and reliability in deep learning," *Neural Computing and Applications*, vol. 37, no. 2, pp. 859–965, 2025.

[37] D. Zhou, Z. Song, Z. Chen, X. Huang, C. Ji, S. Kumari, C.-M. Chen, and S. Kumar, "Advancing explainability of adversarial trained convolutional neural networks for robust engineering applications," *Engineering Applications of Artificial Intelligence*, vol. 140, p. 109681, 2025.

[38] T.-W. Weng, H. Zhang, P.-Y. Chen, J. Yi, D. Su, Y. Gao, C.-J. Hsieh, and L. Daniel, "Evaluating the robustness of neural networks: An extreme value theory approach," *arXiv preprint arXiv:1801.10578*, 2018.

[39] M.-M. Zühlke and D. Kudenko, "Adversarial robustness of neural networks from the perspective of lipschitz calculus: A survey," *ACM Computing Surveys*, vol. 57, no. 6, pp. 1–41, 2025.

[40] M. Fazlyab, T. Entesari, A. Roy, and R. Chellappa, "Certified robustness via dynamic margin maximization and improved lipschitz regularization," *Advances in Neural Information Processing Systems*, vol. 36, pp. 34451–34464, 2023.

[41] M. Dong, Y. Li, Y. Wang, and C. Xu, "Adversarially robust neural architectures," *IEEE Transactions on Pattern Analysis and Machine Intelligence*, 2025.